Quantitative comparison of the OCT imaging depth at 1300 nm and 1600 nm

V. M. Kodach,[1,*] J. Kalkman,[1] D. J. Faber,[1,2] and T. G. van Leeuwen[1,3]

[1]*Biomedical Engineering & Physics, Academic Medical Center, University of Amsterdam, PO Box 22700, 1100 DE Amsterdam, The Netherlands*
[2]*Ophthalmology Department, Academic Medical Center, University of Amsterdam, PO Box 22700, 1100 DE Amsterdam, The Netherlands*
[3]*Biomedical Photonic Imaging, MIRA Institute for Biomedical Technology and Technical Medicine, University of Twente, PO Box 217, 7500 AE Enschede, The Netherlands*
**v.kodach@amc.nl*

Abstract: One of the present challenges in optical coherence tomography (OCT) is the visualization of deeper structural morphology in biological tissues. Owing to a reduced scattering, a larger imaging depth can be achieved by using longer wavelengths. In this work, we analyze the OCT imaging depth at wavelengths around 1300 nm and 1600 nm by comparing the scattering coefficient and OCT imaging depth for a range of Intralipid concentrations at constant water content. We observe an enhanced OCT imaging depth for 1600 nm compared to 1300 nm for Intralipid concentrations larger than 4 vol.%. For higher Intralipid concentrations, the imaging depth enhancement reaches 30%. The ratio of scattering coefficients at the two wavelengths is constant over a large range of scattering coefficients and corresponds to a scattering power of 2.8 ± 0.1. Based on our results we expect for biological tissues an increase of the OCT imaging depth at 1600 nm compared to 1300 nm for samples with high scattering power and low water content.

OCIS codes: (170.4500) Optical coherence tomography; (170.3880) Medical and biological imaging; (290.7050) Turbid media.

References and links

1. D. Huang, E. A. Swanson, C. P. Lin, J. S. Schuman, W. G. Stinson, W. Chang, M. R. Hee, T. Flotte, K. Gregory, C. A. Puliafito, and J. G. Fujimoto, "Optical coherence tomography," Science **254**(5035), 1178–1181 (1991).
2. A. M. Zysk, F. T. Nguyen, A. L. Oldenburg, D. L. Marks, and S. A. Boppart, "Optical coherence tomography: a review of clinical development from bench to bedside," J. Biomed. Opt. **12**(5), 051403 (2007).
3. D. J. Faber, E. G. Mik, M. C. G. Aalders, and T. G. van Leeuwen, "Toward assessment of blood oxygen saturation by spectroscopic optical coherence tomography," Opt. Lett. **30**(9), 1015–1017 (2005).
4. F. J. van der Meer, D. J. Faber, M. C. G. Aalders, and T. G. van Leeuwen, "Identification of plaque constituents using quantitative measurements of tissue optical properties by optical coherence tomography," Eur. Heart J. **24**(5), 152 (2003).
5. M. E. J. van Velthoven, D. J. Faber, F. D. Verbraak, T. G. van Leeuwen, and M. D. de Smet, "Recent developments in optical coherence tomography for imaging the retina," Prog. Retin. Eye Res. **26**(1), 57–77 (2007).
6. A. Unterhuber, B. Povazay, B. Hermann, H. Sattmann, A. Chavez-Pirson, and W. Drexler, "In vivo retinal optical coherence tomography at 1040 nm - enhanced penetration into the choroid," Opt. Express **13**(9), 3252–3258 (2005).
7. B. Považay, B. Hermann, A. Unterhuber, B. Hofer, H. Sattmann, F. Zeiler, J. E. Morgan, C. Falkner-Radler, C. Glittenberg, S. Blinder, and W. Drexler, "Three-dimensional optical coherence tomography at 1050 nm versus 800 nm in retinal pathologies: enhanced performance and choroidal penetration in cataract patients," J. Biomed. Opt. **12**(4), 041211 (2007).
8. J. M. Schmitt, A. Knüttel, M. Yadlowsky, and M. A. Eckhaus, "Optical-coherence tomography of a dense tissue: statistics of attenuation and backscattering," Phys. Med. Biol. **39**(10), 1705–1720 (1994).
9. Y. Yasuno, Y. J. Hong, S. Makita, M. Yamanari, M. Akiba, M. Miura, and T. Yatagai, "In vivo high-contrast imaging of deep posterior eye by 1-μm swept source optical coherence tomography and scattering optical coherence angiography," Opt. Express **15**(10), 6121–6139 (2007).

#129069 - $15.00 USD Received 26 May 2010; revised 2 Jul 2010; accepted 3 Jul 2010; published 16 Jul 2010

10. M. A. Choma, K. Hsu, and J. A. Izatt, "Swept source optical coherence tomography using an all-fiber 1300-nm ring laser source," J. Biomed. Opt. **10**(4), 044009 (2005).
11. G. M. Hale, and M. R. Querry, "Optical constants of water in the 200-nm to 200-µm wavelength region," Appl. Opt. **12**(3), 555–563 (1973).
12. B. E. Bouma, L. E. Nelson, G. J. Tearney, D. J. Jones, M. E. Brezinski, and J. G. Fujimoto, "Optical coherence tomographic imaging of human tissue at 1.55 µm and 1.81 µm using Er- and Tm-Doped Fiber Sources," J. Biomed. Opt. **3**(1), 76–79 (1998).
13. H. Kakuma, K. Ohbayashi, and Y. Arakawa, "Optical imaging of hard and soft dental tissues using discretely swept optical frequency domain reflectometry optical coherence tomography at wavelengths from 1560 to 1600 nm," J. Biomed. Opt. **13**(1), 014012 (2008).
14. U. Sharma, E. W. Chang, and S. H. Yun, "Long-wavelength optical coherence tomography at 1.7 microm for enhanced imaging depth," Opt. Express **16**(24), 19712–19723 (2008).
15. L. Carrion, M. Lestrade, Z. Xu, G. Touma, R. Maciejko, and M. Bertrand, "Comparative study of optical sources in the near infrared for optical coherence tomography applications," J. Biomed. Opt. **12**(1), 014017 (2007).
16. A. W. Sainter, T. A. King, and M. R. Dickinson, "Effect of target biological tissue and choice of light source on penetration depth and resolution in optical coherence tomography," J. Biomed. Opt. **9**(1), 193–199 (2004).
17. J. M. Schmitt, A. Knuttel, and R. F. Bonner, "Measurement of optical properties of biological tissues by low-coherence reflectometry," Appl. Opt. **32**(30), 6032–6042 (1993).
18. D. J. Faber, F. J. van der Meer, M. C. G. Aalders, and T. G. van Leeuwen, "Quantitative measurement of attenuation coefficients of weakly scattering media using optical coherence tomography," Opt. Express **12**(19), 4353–4365 (2004).
19. J. M. Schmitt, S. H. Xiang, and K. M. Yung, "Differential absorption imaging with optical coherence tomography," J. Opt. Soc. Am. A **15**(9), 2288–2296 (1998).
20. Refractive index database, *http://refractiveindex.info*.
21. A. Giusto, R. Saija, M. A. Iatì, P. Denti, F. Borghese, and O. I. Sindoni, "Optical properties of high-density dispersions of particles: application to intralipid solutions," Appl. Opt. **42**(21), 4375–4380 (2003).
22. G. Zaccanti, S. D. Bianco, and F. Martelli, "Measurements of optical properties of high-density media," Appl. Opt. **42**(19), 4023–4030 (2003).
23. J. Kalkman, A. V. Bykov, D. J. Faber, and T. G. van Leeuwen, "Multiple and dependent scattering effects in Doppler optical coherence tomography," Opt. Express **18**(4), 3883–3892 (2010).
24. H. J. van Staveren, C. J. M. Moes, J. van Marie, S. A. Prahl, and M. J. C. van Gemert, "Light scattering in Intralipid-10% in the wavelength range of 400-1100 nm," Appl. Opt. **30**(31), 4507–4514 (1991).
25. C. Chen, J. Q. Lu, H. F. Ding, K. M. Jacobs, Y. Du, and X. H. Hu, "A primary method for determination of optical parameters of turbid samples and application to intralipid between 550 and 1630 nm," Opt. Express **14**(16), 7420–7435 (2006).

1. Introduction

Optical coherence tomography (OCT) is a high resolution, non-invasive, coherence-gated imaging technique with a wide range of applications in medicine [1–5]. One of the present challenges in OCT is the visualization of deeper structural morphology in biological tissues, which can improve existing and create new applications. For current OCT systems the imaging depth is approximately 1–2 mm. The large scattering coefficient of biological tissues limits the amount of light that can be collected from structures located deep in the tissue. Since the optical properties of biological tissues vary significantly with wavelength, the imaging depth can be improved by using a light source with an optimal imaging wavelength.

The general trend for the scattering coefficient is to decrease with increasing wavelength. Therefore, a longer wavelength is potentially more advantageous for deeper imaging. The first OCT system operated in the 800 nm spectral range. The longer wavelength OCT systems, operating in the 1050 nm and 1300 nm spectral bands, were introduced soon after and an improved imaging depth was demonstrated [6–10]. However, the use of longer wavelengths for imaging depth improvement is restricted by the increased optical absorption of water [11]. Nevertheless, the spectral window from 1600 to 1800 nm, between two primary water absorption bands (1400 to 1500 nm and 1900 to 2200 nm), is recognized as a promising choice to further increase the OCT imaging depth. OCT in this part of the spectrum was demonstrated [12–14], and a direct comparison of OCT systems operating at 810, 1330, and 1570 nm was presented [15]. Also, a comparison of light penetration depth for different OCT light sources in skin dermis, liver, and gallbladder was reported [16]. Although these studies have shown that the use of longer wavelengths enables an enhanced imaging depth for certain types of biological tissues, the advantage of using the 1600 – 1800 nm spectral band remains

#129069 - $15.00 USD Received 26 May 2010; revised 2 Jul 2010; accepted 3 Jul 2010; published 16 Jul 2010

to be quantified. Since the different OCT wavelengths were compared based on images that were obtained with different OCT setups, the measured imaging depth depended not only on tissue properties, but also on the technical characteristics of the used OCT systems. In this study, we perform a quantitative comparison of the OCT imaging depth at 1300 nm and 1600 nm wavelengths using a single time-domain OCT set-up of which the technical performance at the two wavelengths is matched. Using Intralipid with a constant absorption coefficient as tissue phantom material, we determine the influence of the scattering on the OCT imaging depth.

2. Materials and methods

2.1 Time-domain optical coherence tomography

The OCT experiments are conducted with a home-built time-domain OCT system. A schematic of the set-up is depicted in Fig. 1(a). Light from a supercontinuum light source (Fianium SC 450-4) is coupled into a single-mode fiber (1550 BHP, Thorlabs) and collimated (FiberPort system, PAF-X-18-PC-C, focal length 18.4 mm, Thorlabs) at the input of a 50/50 Michelson interferometer. In the sample and reference arms, identical achromatic lenses with focal length 45 mm are used to focus the light on the sample and reference mirrors, respectively. Depth scanning is performed by moving the reference arm mirror (at a velocity V = 20 mm/sec), which is mounted together with the lens on a translator (Physik Instrumente M 664.164). In the sample arm, the beam is focused at the front glass-Intralipid interface of the 1 mm thick cuvette. We have fixed focus configuration, i.e the focus position doesn't change during A-scan. The angle between the probe beam and the cuvette is ~70° to avoid specularly reflected light in the signal. Light returning from reference and sample arms is combined and coupled into a single-mode fiber. The interferometric signal is detected with a photodiode (New focus, model 2011), band-pass filtered and demodulated by a lock-in

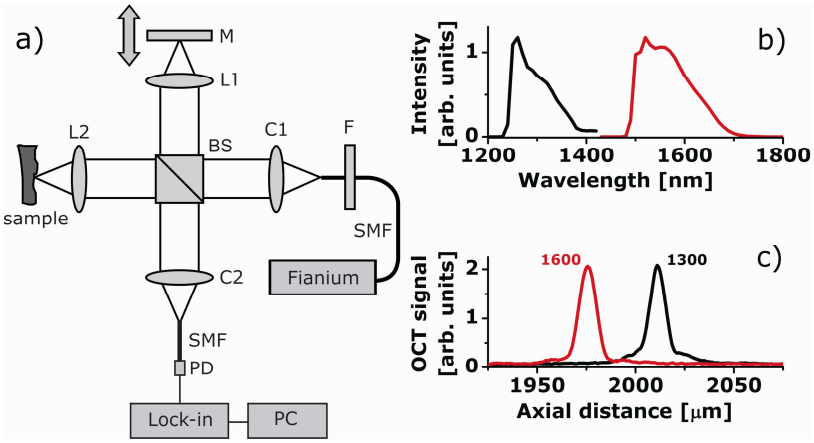

Fig. 1. (a) Overview of the time domain OCT set-up used in the experiments: BS – beamsplitter; C1,C2 - fiber collimating ports; L1, L2 - reference and sample arm lenses; M - reference mirror; SMF - single mode fibers; F - long pass filter; PD - photodetector; Lock-in – Lock-in amplifier; PC - personal computer; Fianium – supercontinuum light source; (b) OCT input spectra for the two wavelength bands; (c) coherence function at the two OCT wavelengths (measured with an OD3 filter in sample arm).

amplifier set to the Doppler frequency $f = 2V/\lambda_0$. To reduce noise, the signal is averaged over 100 A-scans. The sample is not scanned in the lateral direction. The central wavelength λ_0 and the bandwidth of the light coupled into the interferometer is changed between 1300 and 1600 nm bands using long pass filters (Thorlabs, FEL1250 and FEL1500, respectively) and by adjusting the bandwidth of the light coupled to the fiber using the effect of chromatic aberrations [Fig. 1(a)].

#129069 - $15.00 USD Received 26 May 2010; revised 2 Jul 2010; accepted 3 Jul 2010; published 16 Jul 2010

2.2 Performance matched OCT at 1300 nm and 1600 nm

The OCT signal magnitude $i_d(z)$ as a function of depth z is proportional to the square root of the power backscattered from depth z. In the single backscattering approximation and with a coherence length l_c less than the photon mean free path $1/\mu_t$ [17], with μ_t the attenuation coefficient, $i_d(z) \sim P(z)^{1/2} = [P_0\ K\ \mu_b\ h(z)\ \exp(-2\mu_t z)]^{1/2}$ where P_0 is the incident power on the sample; the parameter K is proportional to the coherence length l_c; μ_b is the backscattering coefficient and $h(z)$ is the confocal point spread function (PSF). In the following, we assume either dynamic focusing, or that the data is corrected for the point spread function [18]. The factor of 2 in the exponent accounts for the round-trip attenuation to and from the depth z; the square root accounts for the fact that the OCT signal magnitude is proportional to the amplitude of the field returning from the sample, rather than power.

The OCT signal-to-noise ratio is defined as $SNR = 10\log_{10}(P_0/P_{noise})$, where P_{noise} is the noise power level. We define the imaging depth Z_{image} as the depth at which $P(z) = P_{noise}$, or:

$$Z_{image} = \frac{1}{2\mu_t}\left[Ln\left(K\mu_b\right) + \frac{SNR}{10}Ln10\right] \tag{1}$$

Equation (1) shows that the OCT imaging depth is determined by the optical properties of the sample as well as by the characteristics of the OCT setup itself. For a quantitative comparison of the imaging depth at different center wavelengths only in terms of the optical properties of the sample, it is important to take into account the system characteristics at the two wavelengths.

Firstly the spectral bandwidth of the light coupled into the interferometer [Fig. 1(b)] is adjusted to reach equal coherence lengths of $l_c = 10$ μm at both OCT wavelengths [Fig. 1(c)].

Secondly, the effect of the confocal point spread function on the OCT signal at the two imaging wavelengths is taken into account following the procedure outlined in our previous work [18]. In brief, the change of the OCT signal as a function of distance between the probed location z in the tissue and the focus position z_0 is corrected using the axial PSF, which, in the case of diffuse reflection, has the form: $h(z) = 1/\ \{[(z-z_0)/(2Z_R)]^2 + 1\}$, where Z_R is the Rayleigh length in air. The measured Rayleigh lengths (half the depth of focus) are 0.29 and 0.25 mm at 1300 and 1600 nm, respectively. Due to the achromaticity of the lens, the focus position is different for the two wavelength bands. The positions of the sample arm and reference arm lens are shifted 500 μm when changing from 1300 nm to 1600 nm to compensate for this.

Thirdly, the SNR for a shot-noise limited time-domain OCT system is calculated from the mean square detector current $\langle i_d^2 \rangle$ and the noise variance σ_n^2 as:

$$SNR = 10Log\frac{\left\langle i_d^{\,2}\right\rangle}{\sigma_n^{\,2}} = 10Log\left(\frac{\eta P_s}{E_v \Delta f}\right) \tag{2}$$

where η is the quantum efficiency of the detector, P_s is the power returning from the sample arm; E_v is the photon energy and Δf is the electronic detection bandwidth. The ratio P_s/E_v in Eq. (2) equals the number of photons returning from the sample arm per second. Therefore, the input power is adjusted to obtain an equal amount of photons detected from the sample arm with a mirror positioned at the focus The resulting input powers are 4.5 mW and 6.4 mW for 1300 nm and 1600 nm, respectively, and the power of the light coupled to the detector from the sample arm are 0.33 mW and 0.27 mW, respectively (the optical components have different efficiencies at 1300 and 1600 nm). Since the photon energy at 1300 nm is higher than at 1600 nm, the number of detected photons returning from the sample arm is equal for both OCT wavelengths. Because the quantum efficiency of the photodetector is equal at the two OCT wavelengths, the same signal is measured for the two OCT wavelengths. Although

#129069 - $15.00 USD Received 26 May 2010; revised 2 Jul 2010; accepted 3 Jul 2010; published 16 Jul 2010

our OCT system is not shot-noise limited, the use of the same light source and photodetector ensures that the noise at both wavelengths is matched and an equal SNR is achieved.

Finally, the reference arm power is adjusted using a neutral density filter to optimize the SNR. The lock-in amplifier demodulation frequencies $f = 2V/\lambda_0$ are 30.5 and 25 kHz for 1300 and 1600 nm, respectively, but the detection bandwidth Δf is equal. As a result of the procedure outlined here, the SNR for an OCT measurement with a mirror in the sample arm is equal at the two OCT wavelengths, which we measured to be 90 dB at 1300 and 1600 nm [see Fig. 1(c)].

2.3 Phantom preparation

As a scattering medium we use dilutions of a single batch of 22.7 vol.% (20 weight %) Intralipid (Fresenius-Kabi). Our choice is determined by the fact that Intralipid is a common tissue phantom for optical measurements and it allows us to achieve a high concentration of scatterers. For our measurements Intralipid is diluted to lower concentrations by a mixture of deionized water and heavy water (D_2O). Heavy water has an absorption spectrum similar to water, but the absorption bands are shifted to longer wavelengths [19]. Consequently, heavy water has negligible absorption for wavelengths lower than 1700 nm, which we experimentally verified. The refractive index of D_2O is only slightly different from that of normal water [20], therefore we assume that dilution by heavy water has no significant influence on the scattering properties of Intralipid. The ratio of heavy water and water is such that for all samples the total water concentration (77 vol.%) and, consequently, the absorption is constant, and only the scattering properties vary. We prepared the following samples: 0.7, 1.4, 2.8, 5.7, 8.5, 11.4, 14.2, 17.0, 19.9 and 22.7 volume % Intralipid.

2.4 Determination of optical parameters and imaging depth

OCT measurements at each Intralipid concentration are performed 3 times. For each measurement, 100 A-scans are averaged. Noise background and noise standard deviation are determined from the part of the OCT signal (190 µm) within the first glass wall. After background subtraction, the OCT signal is corrected for the confocal point spread function (dividing the OCT signal by the PSF) [18]. The OCT attenuation coefficient is determined from a single exponential fit of the noise corrected OCT signal in depth: $i_d(z) = a \exp(-\mu_t z)$ with a and μ_t the two free running parameters. The influence of multiple scattering effects is minimized by using only the first 190 µm of the OCT signal for fitting. The OCT imaging depth is calculated from the fit by extending the fitted curve to the point where it intercepts the noise floor (defined as the noise mean plus one standard deviation).

The scattering coefficient of our samples is determined from the measured attenuation coefficient by subtracting the water absorption coefficient from the fitted attenuation coefficient. The variation of the absorption coefficient over the wavelengths of the input spectra is taken into account by calculating the water absorption integrated over the input spectra. We obtain $\mu_a = 0.2$ mm^{-1} and $\mu_a = 1.1$ mm^{-1} for 1300 nm and 1600 nm spectra, respectively. Finally, the standard deviation is calculated from the three subsequent measurements.

3. Results

3.1 OCT signal attenuation

Figure 2 shows averaged OCT A-scans at three different Intralipid concentrations. The OCT signal magnitude at the first glass/Intralipid interface increases with concentration as is expected from the increasing backscattering with increasing particle concentration. The signal magnitudes for 1300 and 1600 nm are approximately equal, which shows that the backscattering coefficient is similar for both cases (the same amount of photons is detected). For the 0.7 vol.% Intralipid concentration, the OCT signal attenuation with depth is lower at

#129069 - $15.00 USD Received 26 May 2010; revised 2 Jul 2010; accepted 3 Jul 2010; published 16 Jul 2010

1300 nm compared to 1600 nm; for the 8.5 vol.% and 22.7 vol.% concentrations the attenuation coefficient is higher at 1300 nm compared to 1600 nm.

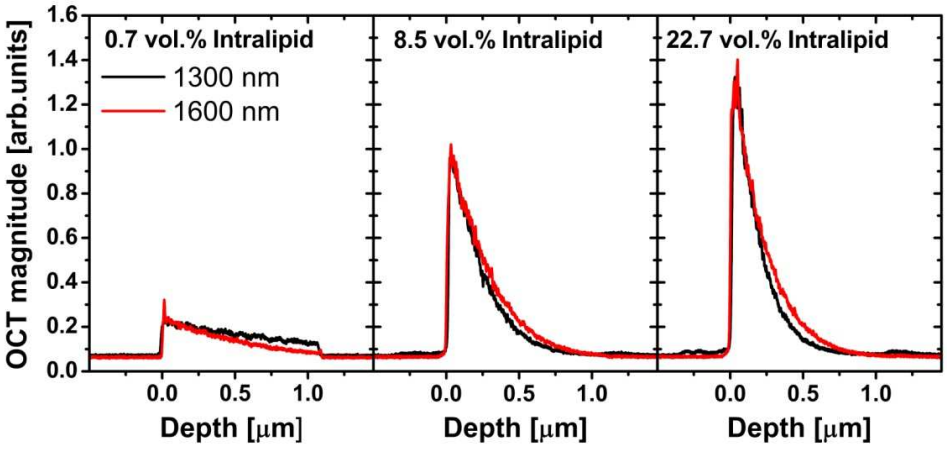

Fig. 2. OCT signals vs. depth for 0.7%, 8.5% and 22.7 vol.% Intralipid samples for the two wavelengths (data before background subtraction and PSF correction).

Figure 3 shows the measured attenuation and resulting scattering coefficient for all Intralipid concentrations. For low Intralipid concentrations the attenuation coefficient is higher at 1600 nm compared to 1300 nm. At Intralipid concentrations larger than ~4 vol.% the attenuation coefficient at 1300 nm exceeds that of 1600 nm. As expected, the scattering coefficient is higher at 1300 nm for all measured Intralipid concentrations. Note that variation of the scattering coefficient with Intralipid concentration shows a clear deviation from the linear dependence expected for low-density media: for high Intralipid concentrations we see a non-linear dependence of the scattering coefficient, which is attributed to concentration dependent scattering [21–23].

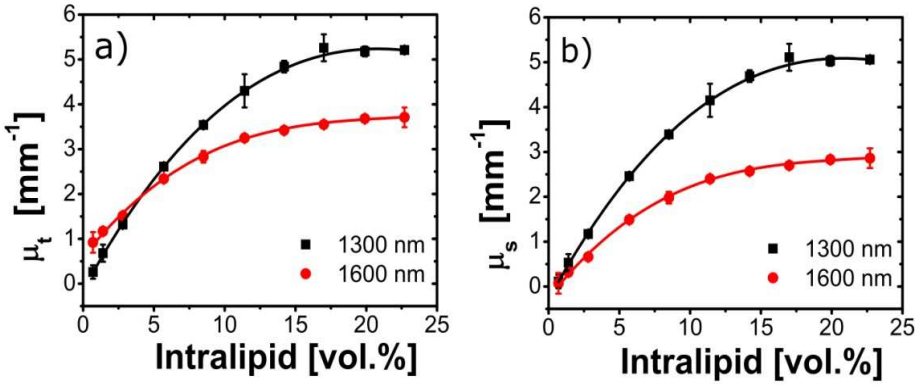

Fig. 3. Measured OCT attenuation (a) and scattering (b) coefficients versus Intralipid concentration. The solid lines are visual guides. Error bars depict standard deviations of the measurements.

3.2 OCT imaging depth comparison

Figure 4 shows the OCT imaging depth for the two OCT wavelengths. At 1300 nm, the imaging depth is larger for low Intralipid concentrations. For example, for the lowest Intralipid concentration (0.7 vol.%) the imaging depth is approximately 3 mm larger for 1300 nm compared to 1600 nm. For 4 vol.% Intralipid the imaging depth at 1600 nm is equal to that

#129069 - $15.00 USD Received 26 May 2010; revised 2 Jul 2010; accepted 3 Jul 2010; published 16 Jul 2010

at 1300 nm. For higher Intralipid concentrations the imaging depth at 1600 nm is larger. At the maximum Intralipid concentration (22.7 vol.%) the OCT imaging depth is 30% larger for 1600 nm compared to 1300 nm (0.8 mm vs 0.6 mm, respectively). In the limit of high Intralipid concentrations the effect of the water absorption on the total attenuation is small at both wavelengths. Consequently, the imaging depth is dominated by the difference in scattering at the two OCT wavelengths.

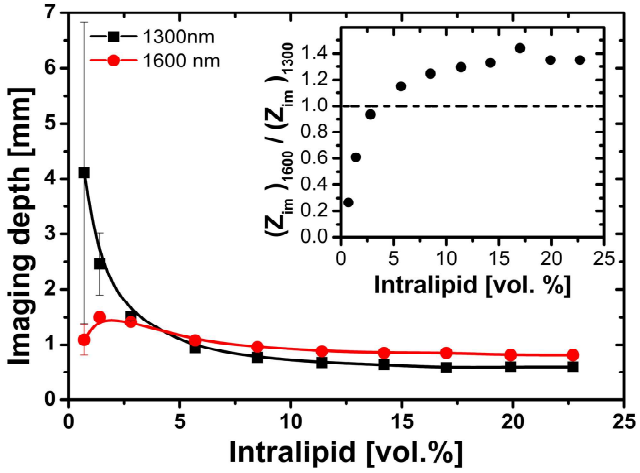

Fig. 4. OCT imaging depth for varying Intralipid concentration measured at 1300 and 1600 nm. The solid lines are visual guides. Error bars depict standard deviations of the measurements. Inset: ratio of measured OCT imaging depths. The dashed line indicates equal imaging depth at 1300 and 1600 nm.

The inset of Fig. 4 shows the ratio of the OCT imaging depth at 1600 nm to that at 1300 nm. For high Intralipid concentrations the imaging depth is dominated by scattering, the ratio of imaging depths is larger than unity. In this limit the 1600 nm OCT wavelength has an approximately 30% larger imaging depth. For low Intralipid concentration, the OCT imaging depth is dominated by absorption, the ratio of imaging depths is smaller than unity and 1300 nm has a larger imaging depth.

It is also interesting to note the dissimilarity of the dependence of the imaging depth at 1300 and 1600 nm on the Intralipid concentration. At 1300 nm it monotonically increases with decreasing Intralipid concentration. The imaging depth at 1600 nm has the same trend, except for low concentrations, where it starts to decrease. This difference can be explained by the stronger contribution of water absorption to the total attenuation coefficient at 1600 nm compared to 1300 nm: for very low Intralipid concentrations the scattering coefficient decreases, resulting in a decreasing backscattering, which lowers the OCT signal amplitude and the remaining high absorption lead to decrease of imaging depth. A similar effect is expected at 1300 nm, but only for very low Intralipid concentrations, not within our measurement range.

4. Discussion

Since the technical characteristics of the OCT setups at 1300 and 1600 nm imaging wavelengths are matched, only the optical properties of the sample determine the difference in the measured OCT imaging depth. In the determination of the OCT imaging depth, two sample parameters are of importance: the backscatter coefficient μ_b, which determines the initial magnitude of the OCT signal, and the attenuation coefficient μ_t, which determines how fast the OCT signal decays with depth to the noise floor.

#129069 - $15.00 USD Received 26 May 2010; revised 2 Jul 2010; accepted 3 Jul 2010; published 16 Jul 2010

The backscatter coefficient μ_b is formally defined as the (total) scattering coefficient of an isotropically scattering particle with a phase function $p_{ISO}(\theta) = p(180)$, where $p(180)$ is the phase function of the original scatterer in the backward direction. This leads to $\mu_b = 4\pi\mu_s\, p(180)$. In the OCT geometry the following interpretation of μ_b is more appropriate: $\mu_b = \mu_s \times \int_{NA} p(\theta) 2\pi \sin\theta d\theta$, e.g. the phase function integrated over the numerical aperture (NA) of the OCT sample arm lens in the backscatter direction. From Eq. (1), the magnitude of the OCT signal immediately after the front glass-Intralipid boundary (z = 0) is therefore proportional to the square root of the scattering coefficient μ_s. Figure 2 shows that the OCT magnitude increases with Intralipid concentration, consistent with the observed increase in the scattering coefficient. In addition, the magnitudes of the OCT signal at 1300 and 1600 nm for the same Intralipid concentration are similar. This suggests that the difference in backscattering coefficient at these wavelengths is small. Since μ_s is larger at 1300 nm compared to 1600 nm [Fig. 3(b)], we conclude that the Intralipid scattering phase function in the backscattering direction (180°) within the detection NA is higher at 1600 nm compared to 1300 nm. This observation is consistent with a reduced size parameter at 1600 nm compared to 1300 nm making the phase function more isotropic at 1600 nm compared to 1300 nm.

Our measurements are performed on samples with constant H_2O content. The reported scattering coefficients are calculated by subtracting a constant absorption from the measured attenuation coefficients [Fig. 3(a)]. Using this method we obtain a μ_s that approaches zero when no scattering is present [zero Intralipid concentration; see Fig. 3(b)]. In addition, the value of the scattering coefficient μ_s at 1300 nm is in good agreement to those found in Ref. [23]. For all Intralipid concentrations the scattering at 1600 nm is lower compared to 1300 nm. However, since the absorption is higher at 1600 nm, the OCT imaging depth is enhanced compared to 1300 nm only for Intralipid concentrations above 4 vol.%. For Intralipid concentrations lower than 4 vol.% the lower scattering coefficient at 1600 is compensated by the higher absorption, resulting in an increased imaging depth for 1300 nm. In the limit of very high Intralipid concentrations the H_2O absorption coefficient can be neglected and the difference between the scattering coefficients at the two wavelengths saturates at $\Delta\mu_s$~2.1 mm^{-1}. Consequently, the OCT imaging depth enhancement also reaches a plateau at a difference of 200 μm, i.e. 30% higher for 1600 nm compared to 1300 nm.

Recent work on the comparison of the performance of OCT systems with light sources centered at 1300 and 1650 nm [14] showed that the ratio of the attenuation coefficients for 10 wt.% Intralipid at 1300 nm to 1650 nm is 1.24. This value is close to our result for this Intralipid concentration, which is 1.29 (with a minor difference in water absorption and central wavelength). However, because of the differences in setup characteristics and the fact that in the published work the attenuation coefficient was calculated without correction for the refractive index of Intralipid, it is difficult to compare our imaging depth measurements with these published results.

It is interesting to compare the scattering coefficient of Intralipid at 1300 and 1600 nm. For a polydisperse solution of particles, like Intralipid, and the absence of strong absorption, the wavelength dependency of the scattering coefficient is described empirically in the form of a power law: $\mu_s = a\lambda^{-SP}$, where a and SP are the parameters for scattering amplitude and scattering power, respectively [24]. The parameter a is associated with the magnitude of the scattering, but does not depend on wavelength: tissues with high scattering coefficient μ_s have high a parameter and vice versa. The SP parameter determines how strong the scattering changes with wavelength. The value of SP is related to the average size of the scatterers: for particles with diameter d much smaller than wavelength of light (d<<λ) the parameter SP approaches 4 (Rayleigh scattering regime). With increasing particles size, the SP decreases (Mie scattering). From this simple model, changes in the scattering coefficient with wavelength (λ_1<λ_2) can be described as follows:

#129069 - $15.00 USD Received 26 May 2010; revised 2 Jul 2010; accepted 3 Jul 2010; published 16 Jul 2010

$$(\mu_s)_{\lambda_2} = \left(\frac{\lambda_1}{\lambda_2}\right)^{SP} (\mu_s)_{\lambda_1} \quad (3)$$

Figure 5 shows the measured scattering coefficient at 1600 nm versus that at 1300 nm for all Intralipid concentrations. From a linear fit to the data points using Eq. (3) we find SP = 2.8 ± 0.1, which is close to a previously reported value of SP for Intralipid SP = 2.4 [24,25]. In addition, Fig. 5 shows that the relative difference in the scattering coefficient at 1300 to 1600 nm remains approximately constant for all Intralipid concentrations. We can conclude that concentration dependent scattering effects are similar for the two wavelengths.

Since the SP parameter describes the wavelength dependence of the scattering coefficient, this parameter can be used to predict changes in the OCT imaging depth with wavelength for biological tissues. From Eq. (3) follows that for samples with a low SP the variation in scattering with wavelength is small. In this case, the increase of the OCT imaging depth with increasing wavelength is expected to be small. For samples with a high SP the scattering coefficient shows a strong variation with wavelength and a relatively large increase of the OCT imaging depth can be expected. Additionally, for samples with significant water content, the higher water absorption in the 1600 – 1800 nm spectral band is a counteracting factor. Therefore, we expect an increase of the OCT imaging depth for samples with high SP and low water content (e.g. enamel) and we do not expect an increase of the OCT imaging depth for samples with a low SP and high water content (e.g. skin). However, since the wavelength dependence of the backscattering coefficient is not known a priori, the procedures, as outlined in this paper, should be followed to determine the optimum OCT imaging wavelength.

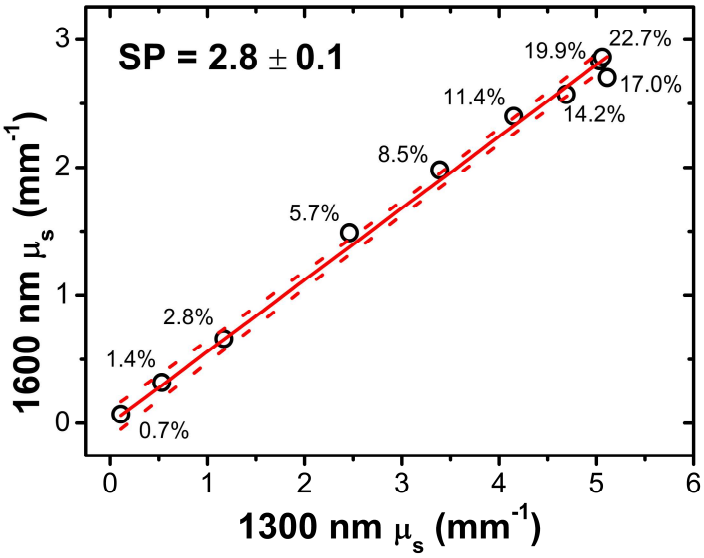

Fig. 5. Measured μ_s at 1600 nm versus 1300 nm. Sample points are marked according to the Intralipid concentration. From a linear fit to the data (solid line) we determine the SP value for Intralipid (indicated). The dashed lines indicate the 95% confidence interval of the fit.

5. Conclusions

We present a quantitative comparison of the OCT imaging depth in Intralipid (with constant water content of 77 vol.%) at 1300 and 1600 nm. For Intralipid concentrations larger than 4 vol.% the imaging depth at 1600 nm becomes larger than for 1300 nm. We show that for high Intralipid concentrations the use of 1600 nm light gives a 30% larger OCT imaging depth compared to 1300 nm. Despite concentration dependent scattering effects, the ratio of scattering coefficients at the two wavelengths is constant. Additionally, we observe that

#129069 - $15.00 USD Received 26 May 2010; revised 2 Jul 2010; accepted 3 Jul 2010; published 16 Jul 2010

difference in the backscattering at these wavelengths is small, which suggests that the backscattering phase function at 1600 nm is higher than at 1300 nm. Regarding application to biological tissues, an increase of the OCT imaging depth at 1600 nm for samples with a high scattering power parameter and low water content is expected.

Acknowledgments

V. M. Kodach and J. Kalkman are supported by the IOP Photonic Devices program (IPD067774) managed by the Technology Foundation STW and SenterNovem. D. J. Faber is funded by a personal grant in the Vernieuwingsimpuls program by the Netherlands Organization of Scientific Research (NWO) and the Technology Foundation STW (AGT07544).